

# Embedded Slot Antenna with V-Slot DGS

<sup>#</sup>M. Esa, M. S. Awang, N. N. N. A. Malik, N. M. A. Latiff, R. Arsat, and N. A. Samsuri  
Faculty of Electrical Engineering, Universiti Teknologi Malaysia,  
81310 UTM Johor Bahru, Johor, Malaysia, mazlina@fke.utm.my

## 1. Introduction

The performance of microstrip patch antenna can be improved by employing a technique to improve that involves defected ground structure (DGS) [1]-[4]. DGS provides slow wave effect in the frequency below band-gap and fast-wave effect above the band-gap frequency [5]. DGS adds an extra lumped capacitance and inductance to the distributed line. A major benefit is the ability to reduce undesired cross-polarisations. The technique has been proven to improve some characteristics of the antenna for certain applications such as reduce mutual coupling in a microstrip array, and reduce cross polarisation radiation on a single element. Simple design structures are etched on the ground plane of the antenna. This will disturb the current distribution that will simultaneously improve the performance of the antenna. In this paper, the design of a microstrip slot antenna [6] is modified by having DGS element embedded in the ground plane. The DGS has the shape of a V-slot. Both antennas with and without the DGS element have been successfully simulated and measured. It was found that the microstrip slot antenna with V-slot DGS outperforms its counterpart in terms of suppressed cross-polarisation and broadened impedance bandwidth. The antennas are named as WA and WAV antenna sets. The effects of introducing the V-slot DGS onto WA's ground plane have been successfully investigated [7].

## 2. Design Considerations of Embedded Slot Antenna

The desired operating frequency,  $f_0 = 5.8$  GHz is chosen for WLAN application [8]. The corresponding wavelength,  $\lambda_0 = 51.7241$  mm. Low loss RT/Duroid 5870 microwave board is used. It has relative permittivity,  $\epsilon_r = 2.33$ , loss tangent = 0.0012, and thickness of the substrate,  $h = 1.575$  mm. The chosen feed technique is electromagnetic coupling. Firstly, the sides of the square patch are designed using the equation available in the literature [8], [9];

$$W = \frac{c}{2f_o} \left( \frac{\epsilon_r + 1}{2} \right) \quad (1)$$

Hence, the calculated width dimension is  $\sim 33.4$  mm. The corresponding bandwidth of the antenna is calculated using the equation available in [8],[9]:

$$BW = \frac{f_H - f_L}{f_o} \quad (2)$$

The optimum conventional square patch antenna is then obtained through EM simulations [10]. Then, a rhombus shaped slot is introduced in the middle of the radiating patch. It is added so as to broaden the impedance bandwidth of the antenna [6]. However, the cross-polarisation remains high. Next, the antenna is simulated for optimisation. Then, a short strip is introduced into the wideband antenna in order to improve the impedance match [1]. Finally, a unique DGS element named V-slot, is integrated for the purpose of reducing the undesired high cross-polarisation. Fig. 1 shows the cross-sectional view and prototype of the proposed antenna.

Through simulations, the optimised dimension of the conventional patch is 35 mm X 35 mm, the optimised slot is 17.5 mm X 17.5 mm, whilst the optimised short strip is 8 mm X 3 mm. The 50 ohm feed line is 35 mm long and 3 mm wide. The sizes of upper and lower boards are 45 mm X 45. The location of the EMC feed corresponds to an input impedance of 50 ohms at resonance, indicating excellent impedance match at the input. The location was computed using equations from [9] for the square patch antenna. This is then optimised through EM simulations when the rhombic slot and short strip are introduced.

A DGS slot is then embedded into the ground plane of the WA antenna. General circuit model for modelling a wide range of DGS structure is available in [11]. Variations of the DGS slot are then introduced in order to optimise the antenna performance, particularly in suppressing the undesired inherent cross-polarisation. Finally, the feed is fine tuned when the DGS is embedded. The WA and WA antennas were simulated for their return loss behaviours. The final optimised performances are comparable to [12].

### 3. Performances of the Designed Antennas

The simulated and measured return loss responses of the WA and WAV antennas are shown in Figs. 3 to 5. The simulated and measured E-plane radiation patterns of the WA and WAV antennas are depicted in Figs. 6 to 8, and 9, respectively.

It can be observed that WA exhibits wide -10 dB operating bandwidth from 5.55 GHz to 8.14 GHz. For WAV, impedance bandwidth slightly increased to 40 %, as expected. However, the operating bandwidth slightly shifted upwards to the range from 5.577 GHz to 8.344 GHz. The range has four dips at 5.877 GHz, 6.625 GHz, 7.363 GHz and 8.101 GHz. It can be inferred that there is slight increase of antenna size at the upper frequency edge. The shift may be attributed to the change of the input reactance of the dominant mode under the patch caused by significant introduced defects on the ground plane [1],[12].

From the measured return loss responses, it can be observed the -10 dB operating bandwidth of the WA is from 5.7 GHz to 8.7 GHz or ~42 %. There is a slight improvement to the range 5.5 to 8.7 GHz or 45%. Good agreement is observed between the simulation and measurement results. Hence, it can be inferred that the DGS has improved the impedance bandwidth of both antennas by 2 % and 3 %, respectively. The observations are similar to [1].

The selected simulation results at 5.8 GHz and 6.9 GHz showed that the corresponding E-plane co- and cross-polarisations of each antenna are identical. However, the isolation is large enough. The E-plane cross-polarisation levels of the WAV antennas have dropped. The reduction agrees well with [3]. In addition, the E-plane HPBW has greatly reduced from 54.86° to 33.07°, thus making the WAV more directive.

The selected measured results at 5.95 GHz and 7 GHz showed that the corresponding E-plane co- and cross-polarisation of each antenna are similar, and agree well with [1], [2]. The measured E-plane cross-polarisation of WA has greatly dropped when V-slot DGS is introduced. The cross-polarisation level dropped from -60 dBm to -70 dBm. The corresponding cross-polarisation reduction is ~10 dBm.

Both the simulation and measurement results have been presented for selected frequencies of operations within the operating bandwidth. Both results showed reduction in cross-polarisation levels, despite slight disagreement of the E-plane cross-polarisation levels. This could be due to simulation inaccuracies and fabrication errors.

### 4. Conclusions and Further Work

The design of a wideband microstrip antenna that is embedded with DGS element of V-shaped slot has been presented. The antenna is compared with its basic counterpart. Both antennas have been successfully simulated and measured. It was found that the undesired cross-polarisation has been reduced and the impedance bandwidth is slightly broadened. The defect on the ground plane has disturbed the current distribution in the ground plane, which affected the capacitance and inductance of the antenna, thus perturbing and suppressing the occurrence of any orthogonal resonance [1]. Slight disagreement of the E-plane cross-polarisation level is observed for the WA. Nevertheless, the experimental results confirmed that the DGS V-slot has successfully improved the isolation of the E-plane co- and cross-polarisation radiation patterns.

### Acknowledgments

The authors acknowledge the support of Universiti Teknologi Malaysia and Malaysia Government.

## References

- [1] Debatosh Guha, Manotosh Biswas and Yahia M. M. Antar, "Microstrip Patch Antenna with Defected Ground Structure for Cross Polarization Suppression", *IEEE Antennas and Wireless Propagation Letters*, vol. 4, pp. 455-458, 2005.
- [2] Zhi Ning Chen, Max J. Ammann, Xianming Qing, Xuan Hui Wu, Terence S. P. See, and Ailian Cai, "Planar Antenna" *IEEE Microwave Magazine*, Dec. 2006. vol. 7, no. 6, pp. 1-73.
- [3] Wen-Hsiu Hsu and Kin-Lu Wong, "Broad-Band Probe-Fed Patch Antenna with a U-Shaped Ground Plane for Cross-Polarization Reduction", *IEEE Trans. on Ant. and Propagat.*, Vol. 50, No. 3, pp. 352-355, March 2002.
- [4] S. S. Iqbal, J. Y. Siddiqui and D. Guha, "Performance of compact integratable broadband microstrip antenna", *Electromagnetics*, vol. 25, no. 4, pp. 317-327, May/June. 2005.
- [5] Hyung-Mi. Kim and Bomson Lee, "Bandgap and slow/fast wave characteristics of defected ground structures (DGSs) including left-handed features", *The Transaction on Microwave Theory and Techniques*, vol. 54, No. 7, July 2006
- [6] V. P. Sarin, Nisha Nassar, V. Deepu, C. K. Aanandan, P. Monahan and Kesavath Vasudevan, "Wideband Printed Microstrip Antenna for Wireless Communications", *IEEE Antennas and Wireless Propagation Letter*, vol. 8, 2009.
- [7] M. S. Awang, *Embedded Antenna with Reduced Polarizations*, unpublished dissertation, Universiti Teknologi Malaysia, Nov. 2009.
- [8] K. L. Wong, *Compact and broadband Microstrip Antennas*. New York: Wiley, 2002
- [9] C. A. Balanis, *Antenna Theory and Design*, New York: Wiley, 3<sup>rd</sup> edn, 2005.
- [10] <http://www.sonnetusa.com>
- [11] Jia-Sheng Hong and Bindu M. Karyamapudi, "A General Circuit Model for Defected Ground Structures in Planar Transmission Lines", *IEEE Microwave and Wireless Components Letters*, vol 15, No. 10, pp. 706-708, 2005.
- [12] S. Noghianian and L. Shafai, "Control of microstrip antenna radiation characteristics by ground plane size and shape", *IEE Proc-Microw. Ant. Prop.*, vol. 145, no. 3, pp. 207-212, June 1998.

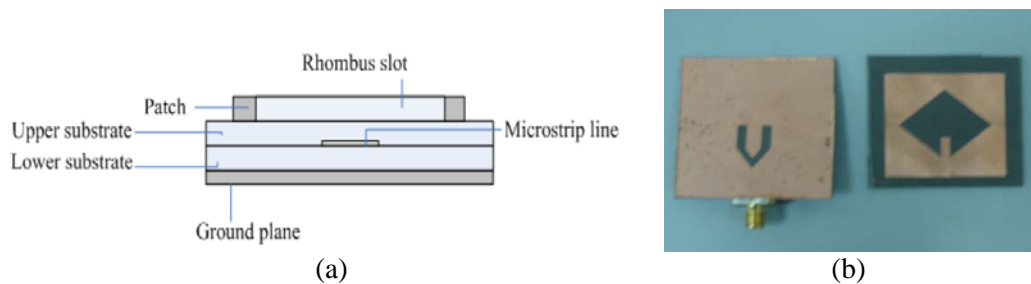


Figure 1: WAV Antenna (a) cross-sectional view (b) V-slot DGS (left) and radiating patch (right).

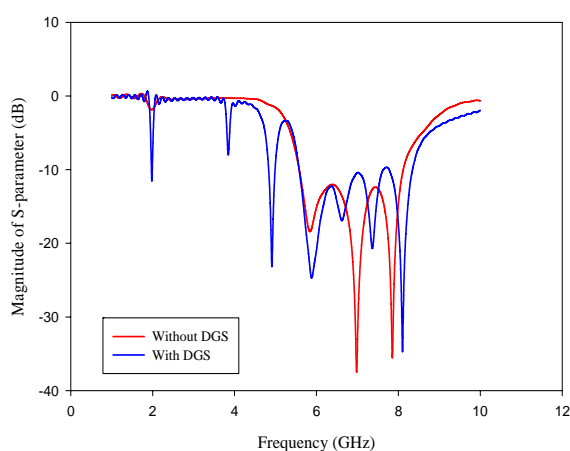


Figure 2: Simulated Return Loss Responses of WA and WAV Antennas.

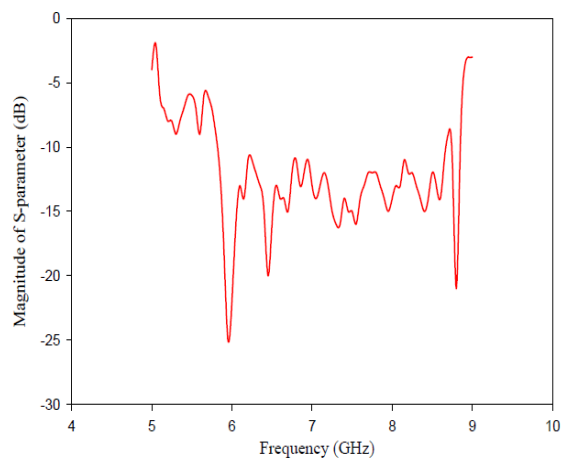


Figure 3: Measured Return Loss Response of WA Antenna.

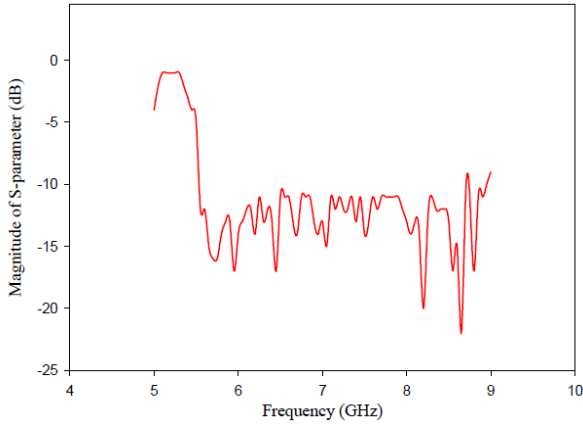


Figure 4: Measured Return Loss Response of WAV Antenna.

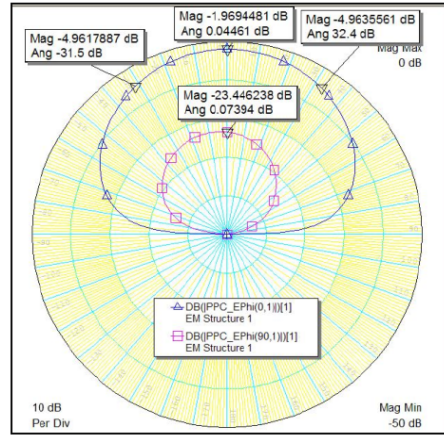


Figure 5: Simulated E-Plane Radiation Patterns of WA Antenna at 5.8 GHz.

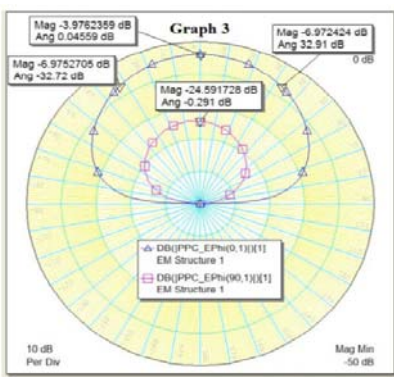


Figure 6: Simulated E-Plane Radiation Patterns of WAV Antenna at 5.8 GHz

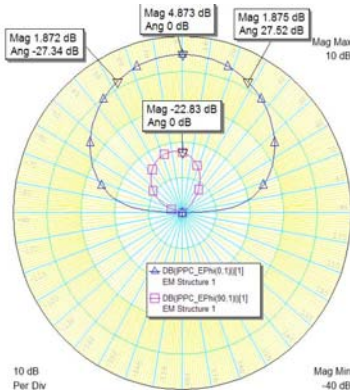


Figure 7: Simulated E-Plane Radiation Patterns of WA Antenna at 6.9 GHz

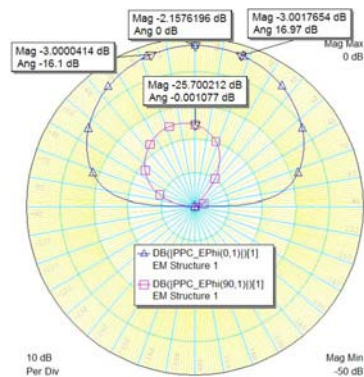
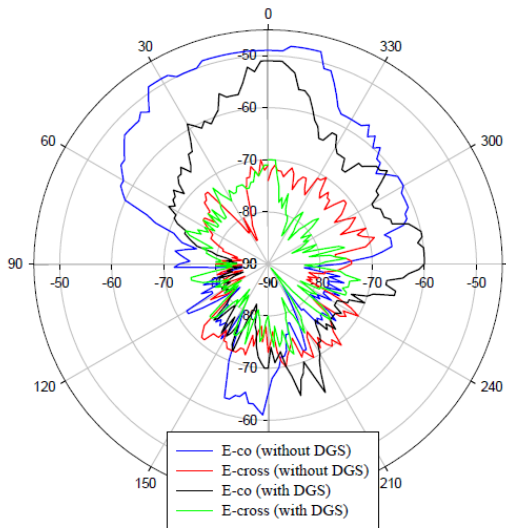
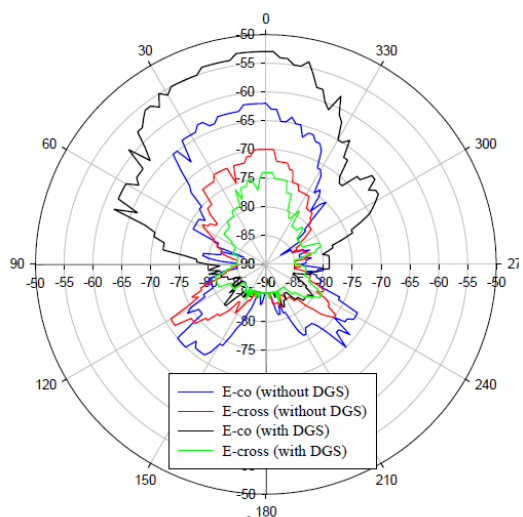


Figure 8: Simulated E-Plane Radiation Patterns of WAV Antenna at 6.9 GHz



(a)



(b)

Figure 9: Measured E-Plane Radiation Patterns of WA and WAV Antennas at (a) 5.95 GHz (b) 7 GHz